

## Effect of MAO-modified nanoporous silica supports with single-site titanocene catalyst on ethylene polymerization

Farideh Azimfar\*, Alireza Badiel\*\*,†, Seyed Mehdi Ghafelebashi\*\*\*, Majid Daftari-Besheli\*\*\*, and Abbas Rezaee Shirin-Abadi\*\*\*\*

\*School of Chemistry, Alborz Campus, University of Tehran, Tehran, Iran

\*\*School of Chemistry, College of Science, University of Tehran, Tehran, Iran

\*\*\*National Petrochemical Company, Petrochemical Research and Technology Company, P. O. Box 1435884711, Tehran, Iran

\*\*\*\*Faculty of Chemistry & Petroleum Sciences, Department of Polymer & Materials Chemistry,

Shahid Beheshti University, G.C., 1983969411 Tehran, Iran

(Received 21 June 2017 • accepted 3 December 2017)

**Abstract**—Three types of nanoporous silica support were modified by methylaluminoxane MAO and characterized by using BET, SEM, XRD and TGA. Dimethylsilyl (N-tert-butylamido)(tetramethylcyclopentadienyl) titanium dichloride was synthesized and immobilized on modified support. The prepared complex was then used as a reactive catalyst for ethylene polymerization. The effect of immobilization conditions on catalyst performance was studied. The results revealed elevated temperature grafting, decrease in precatalyst loading. Also, increasing of immobilization reaction time showed an increase in activity to 130 Kg poly/mol Ti.h.bar. The effects of polymerization temperature and [Al]/[Ti] ratio on the catalyst behavior, namely activity and bulk density, were investigated. According to the results, the activity of single-site catalyst depends on condition of immobilization and structure of nanoporous silica support.

Keywords: Nanoporous Silica, Titanocene, Immobilization, Polymerization, Polyethylene (PE)

### INTRODUCTION

The discovery of metallocene and single-site catalysts for olefin polymerization exhibits many interesting characteristics of produced polymer through the rational design of ligands and the structure of related complexes [1-8]. It also offers wide flexibility range along with control on polymer properties in comparison with conventional Ziegler-Natta catalysts [9]. Constrained geometry catalysts (CGCs) (Insite technology,  $\text{Me}_2\text{Si}(\text{C}_5\text{Me}_4)(\text{N-tBu})\text{TiCl}_2$ ), are a new generation of metallocenes which have found wide range of interests both in academia and industry since the 1990s [10-14]. Common types of CGC catalysts retain one of the cyclopentadienyl rings of metallocenes, but replace the other ring with a nitrogen substituent which is able to coordinate with the metals [13,15]. The amide donor ligand in the structure of these types of complexes stabilizes the electrophilic metal center, while the short  $\text{Me}_2\text{Si}$ -bridging group creates more space at the metal site environment compared to conventional metallocenes [16]. This unique structure allows excellent control of the polymer chain structures and production of polymer with high efficiency and value added [17-20]. Although several experimental studies on olefin homo and copolymerization with CGCs have been published [10-14], the preparation of supported single-site catalysts is indeed a big challenge, mostly because the polymer morphology must be controlled in such a way that characteristics of molecular catalysts are retained [21]. Despite the

numerous advantages of metallocene and single-site catalysts, some issues such as control on polymer morphology, thermal stability of the catalysts and adaptability to various commercial processes such as slurry and gas phase processes, still need to be addressed. To fulfill these requirements, immobilization of the catalysts on various carriers especially silica to make a “drop-in” process, has been an important topic for researchers [6]. One of the most important keys in immobilization is to ensure fine control of the surface chemistry of the support as well as procedure which is used to produce the methylaluminoxane (MAO) activated silica support [22,23]. Several methods have been reported for immobilization of metallocene catalysts but the most widely used method is to treat a silica surface containing surface silanol groups with MAO before addition of metallocene catalyst to make a catalytic complex with the surface-anchored MAO [24-26].

In this research, nanoporous silica support was modified with MAO. The dimethylsilyl (N-tert-butylamido)(tetramethylcyclopentadienyl) titanium dichloride (Fig. 1) was synthesized and immobilized on modified support, and was then used as catalyst for ethylene polymerization. The influence of some critical parameters such as

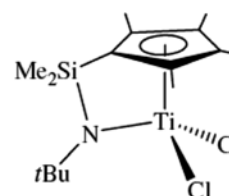


Fig. 1. Structure of CGC catalyst used in this study.

†To whom correspondence should be addressed.

E-mail: abadie@khayam.ut.ac.ir

Copyright by The Korean Institute of Chemical Engineers.

silica type and immobilization conditions including temperature and time of immobilization on catalyst performance was studied. The polymerization behavior at various conditions such as different temperature and [Al]/[Ti] ratio was also studied.

## MATERIAL AND METHODS

### 1. Materials

All methods and manipulations involving air or water sensitive compounds were handled under inert atmosphere in a glove box. MAO (10 wt% in toluene) was purchased from Aldrich (USA) and used without further purification. Polymer grade ethylene with high purity was obtained from Bandar Imam Petrochemical Corporation (Iran) and further purified by passing through an oxygen/moisture trap. Silica Grace Davisil 643 and 633 were purchased from Aldrich Company and the synthesized silica sample was denoted by NPC-RT Company (Iran). The silica supports were dried under nitrogen flow prior to use. Toluene for polymerization was supplied from Merck Company and was refluxed in the presence of sodium/benzophenone and distilled prior to use (the water content was lower than 5 ppm by Karl-Fischer titration). The catalytic precursor dimethylsilyl (N-tert-butylamido)(tetramethylcyclopentadienyl) titanium dichloride was synthesized according to previously reported procedure [27].

### 2. Catalyst Preparation

#### 2-1. Preparation of Synthesized Silica

Silica support was prepared using alkaline solution of sodium silicate by sol-gel method. The first 30 ml sodium silicate with 25 ml of deionized water was mixed and 35 ml of sulfuric acid 12.5% by weight over a period of 105 minutes by stirring was added. After addition, acid was separated from the ice bath (without performing aging stage), and sodium ion from silica hydrogel by washing with aqueous ammonium nitrate solution was removed. Dry powder silica was obtained at 550 °C.

#### 2-2. Pretreatment of Silica with MAO

Silica was dried under nitrogen flow prior to use at 350 °C for 6 h (calcination). In a round-bottom flask, 3 g of dried silica was stirred in toluene and then 7 ml of MAO solution (10 wt% in toluene) was added drop-wise in 30 min at room temperature. Then the reaction temperature was set to 70 °C and allowed to be stirred for 18 h. The resulted suspension containing silica was filtered and washed with 400 mL of dried toluene for 8 to 10 times to remove the unreacted aluminum. Finally modified silica was dried under vacuum at room temperature.

#### 2-3. Preparation of Immobilized Titanocene Catalyst on Silica

A typical procedure for immobilization of dimethylsilyl (N-tert-

butylamido)(tetramethylcyclopentadienyl) titanium dichloride on silica was as follows. In a 250 mL round-bottom flask, 2.6 g of silica pretreated with MAO from the previous section was introduced and stirred in 10 mL of toluene. Then, 0.12 g of precatalyst was dissolved in 6 mL of toluene and transferred to pretreated of silica with MAO using syringe at room temperature. The catalyst mixture was heated to 50-70 °C and stirred for 3-18 h. The obtained catalyst was filtered and washed with toluene and dried under vacuum at room temperature.

### 3. Ethylene Polymerization

For ethylene polymerization a 1 L stainless steel reactor was used. The reactor, which was equipped with a magnetic stirrer, was degassed and filled with nitrogen, toluene (500 mL), and MAO solution (400 mg) as scavenger was introduced to the reactor and stirred at 400 rpm for 15 min. A certain amount of MAO as activator was added to the reactor, and after 15 minutes the appropriate amount of catalyst was introduced. The reactor was pressurized with ethylene and the pressure reached 8.0 bar. Then the vessel was warmed to the desired polymerization temperature. After the polymerization (1 h), excess ethylene was vented off and the polymerization quenched by adding acidified ethanol. The polymer was filtered, washed extensively with ethanol and dried at 40 °C in an oven overnight to reach a constant weight.

### 4. Characterization

The metal content of the immobilized catalysts was determined by inductively coupled plasma (ICP). Scanning electron microscopy (SEM) was used to determine the morphology of silica supports, catalyst and polymer. SEM images were obtained with Vega-Tescan (Czech Republic) electron microscope. The elemental mapping images were taken from Philips instrument (XL30), under vacuum, accelerated at 20 kV. X-ray diffraction (XRD) was used to determine the bulk crystalline phases of samples. Diffraction patterns were obtained using a Siemens Diffraktometer D500 instrument. Thermogravimetric analysis (TGA) was used for evaluation of thermal stability of the silica and the measurements were done by a Perkin Elmer Pyris Diamond. BET surface area, average pore diameter and pore size distribution were measured by N<sub>2</sub> physisorption using NOVA 2000 Quantachrome (USA) system. Differential scanning calorimetry (DSC) tests were recorded on a Mettler-Toledo (Switzerland) model 822e instrument, at a heating/cooling rate of 10 °C min<sup>-1</sup>, under nitrogen flow. Gel permeation chromatography (GPC) was performed by Varian (PL-GPC220) at 145 °C in trichlorobenzene with polystyrene standards. Powder bulk density (BD) of samples were measured based on the industrial standard procedures ASTM D1895-69. Particle size distribution of polymers was characterized by Mastersizer 2000, Malvern.

**Table 1. The influence of structure of support on the catalyst system<sup>a</sup>**

No.	Silica	Surface area (m <sup>2</sup> /g)	Pore volume (cm <sup>3</sup> /g)	Average pore diameter (Å)	Average particle size support (μm)	Average particle size polymer (μm)	Bulk density (g/mL)	Activity (kg poly/molTi.h.bar)
1	Davisil 643	276	1.10	150	55	415	0.32	130
2	Synthesized	204	0.75	130	64	30	0.11	87
3	Davisil 633	493	0.86	60	52	155	0.20	97
4	Homogeneous	-	-	-	-	75	0.26	520

<sup>a</sup>T=75 °C, P=8 bar, Al/Ti=450 (molar ratio)

Calcinations condition: T=350 °C, t=6 h

## RESULTS AND DISCUSSION

Four series of experiments were conducted to evaluate the performance of prepared catalyst system in ethylene polymerization: (1) the pore characteristics of various silica supports; (2) the catalytic activity of metallocene catalyst systems prepared using the supports; (3) the loading of activator and metallocene on to the support; and (4) the properties of produced polymers from polymerization reaction which is catalyzed by the above prepared metallocene catalyst system. Three kinds of silica samples were employed in this study and their specification is summarized in Table 1. All three silicas had total surface areas of at least  $\sim 200 \text{ m}^2/\text{g}$  and pore volume of at least  $\sim 0.75 \text{ cm}^3/\text{g}$ . The average support particle size ranged from 52 to 64 micrometers.

### 1. Effect of Support Structure on the Catalyst System

It has been reported that the activity usually decreases by immobilization of the catalyst on the support [28]. The type and the structure of support would have an important impact on performance of metallocene catalyst. The sufficiently large pore diameter of silica allows metallocene to diffuse and interact efficiently with inner surface of the support. At the same time, the pore volume must not be too large in order to decrease the surface area for activator-metallocene-support interactions, or to create too fragile a metallocene catalyst system. Such that it does not remain intact during the process for formation of the metallocene catalyst system or during the metallocene catalyst system's transport to a reactor.

Table 1 shows that synthesized silica and Davisil 633 have low total pore volume; most of the pores have diameters of less than  $150 \text{ \AA}$ . It has been reported that in silicas with pore diameter smaller than  $100 \text{ \AA}$ , the negative curvature keeps silanol groups closer, favoring the formation of hydrogen bonds and therefore, increasing the stability of silanol groups against dehydroxylation, which leads to a decrease in catalyst activity [25]. Table 1 also shows that although Davisil 633 has a high total surface area, most of the surface area is allotted to small pores with diameters of less than  $150 \text{ \AA}$ .

The highest catalyst activity was observed for the catalyst using Davisil 643 support which was commercial silica and the lowest activity obtained with the supported system immobilized on the synthesized silica. This observation could be most likely attributed to the pore volume and pore diameter of Davisil 643, which allows greater amounts of metallocene to be bound and activated in the interior pores in this support compared to synthesized support. Although Davisil 633 has small pore diameter, its catalyst activity is more than catalyst system including synthesized silica due to its higher pore volume and surface area (Table 1).

SEM images of silica supports are depicted in Fig. 2. It can be seen that the physical surface of synthesized silica is frangible. The produced polymer by using system with synthesized silica support has the lowest particle size in comparison to other systems including Davisil 643 and Davisil 633 (see Table 1). The frangible structure of synthesized silica and its catalyst also leads to very low bulk density.

Thermal behavior of noncalcinated silica samples was studied by using TGA under inert atmosphere, and results are in Fig. 3. The trend of weight loss for Davisil 643 and Davisil 633 was similar. There is a steep weight loss at about  $100^\circ\text{C}$  that most likely is

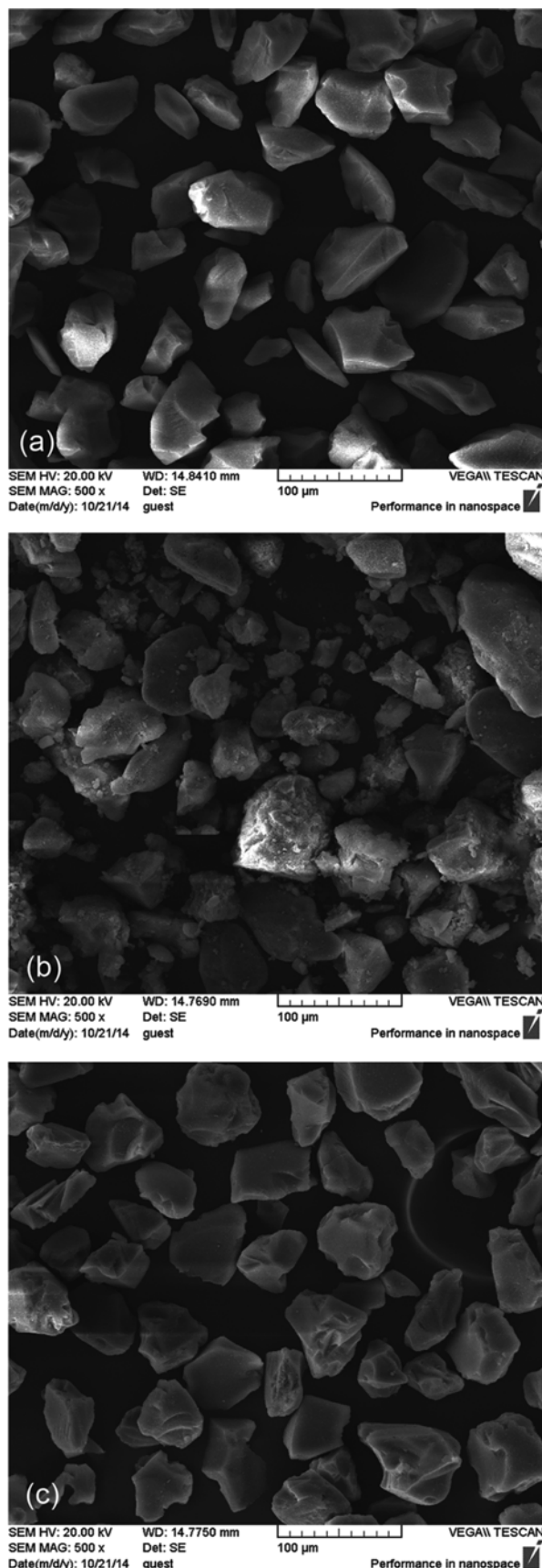


Fig. 2. SEM images of silica supports which are used for CGC catalyst, Davisil 643 (a), synthesized silica (b), and Davisil 633 (c).

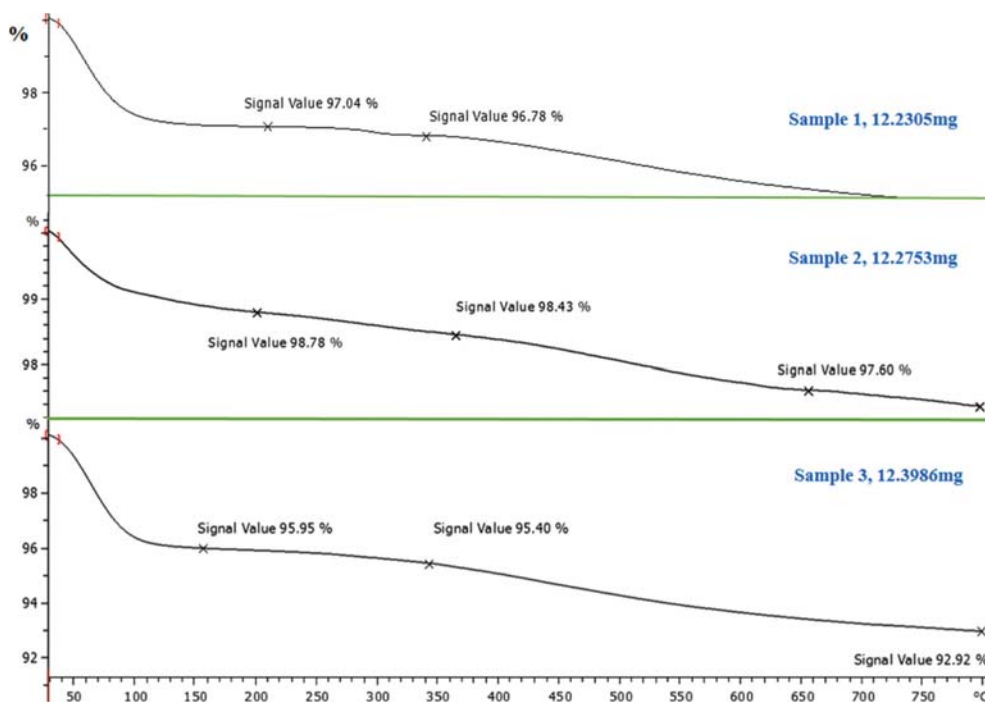


Fig. 3. TGA graph of silica support Davisil 643 (1), synthesized silica (2) and Davisil 633 (3).

associated with the loss of OH groups. The observed weight loss is about 3 percent. Increasing temperatures to 750 °C led to weight loss of about 5-7% with a mild slope (Fig. 3(1), (3)). Davisil 633 in comparison with synthesized silica loses ~2% more, due to its higher surface area and in consequence higher amount of OH groups. The weight losses of synthesized silica with the least surface area were about 1% and 3% at 100 °C and 750 °C, respectively. Therefore, less reduction in OH groups led to decrease in loading of precatalyst and catalyst activity.

Fig. 4 shows an X-ray powder diffraction pattern of silica samples. An amorphous peak with the equivalent Bragg angle at  $2\theta = 26.04$ ,  $24.80$  and  $25.18$  degrees was recorded for Davisil 643, Synthesized silica and Davisil 633, respectively. This peak was related to the amorphous phase and was existent on heating silica up to 800 °C. Overheated amorphous silica at 1,000 °C, tetragonal  $\alpha$ -cristobalite and a small fraction of monoclinic tridymite were received [30].

## 2. Effect of Calcination Temperature on Catalyst Activity

Due to better characteristics of silica Davisil 643, it was chosen

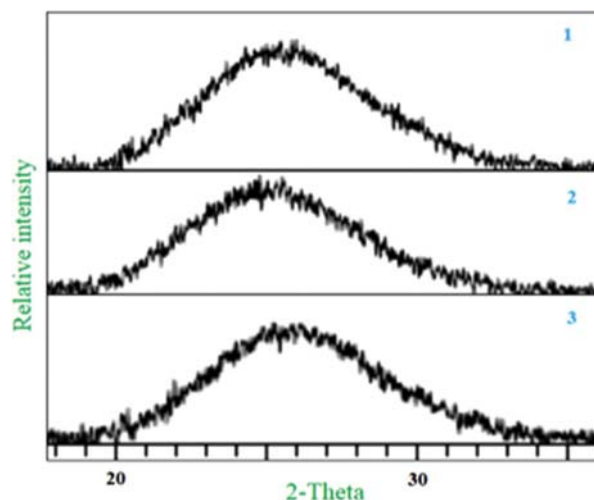


Fig. 4. XRD patterns of silica Davisil 643 (1), synthesized silica (2), Davisil 633 (3) with a characteristic amorphous peak.

Table 2. Variable studied parameters on immobilization of  $(C_5Me_4SiMe_2NtBu)TiCl_2$  on Davisil 643<sup>a</sup>

No.	T (immobilization) (°C)	t (immobilization) (h)	%Ti	%Al	T (calcination) (°C)	Activity (kg poly/molTi.h.bar)
1	50	18	0.12	3.28	350	109
2	60	3	0.10	3.12	350	83
3	60	6	0.14	3.31	350	102
4	60	18	0.15	1.62	600	96
5	60	18	0.23	3.81	350	130
6	70	18	0.19	3.70	350	114

<sup>a</sup>Polymerization condition: T=75 °C, P=8 bar, Al/Ti=450 (molar ratio), solvent: toluene

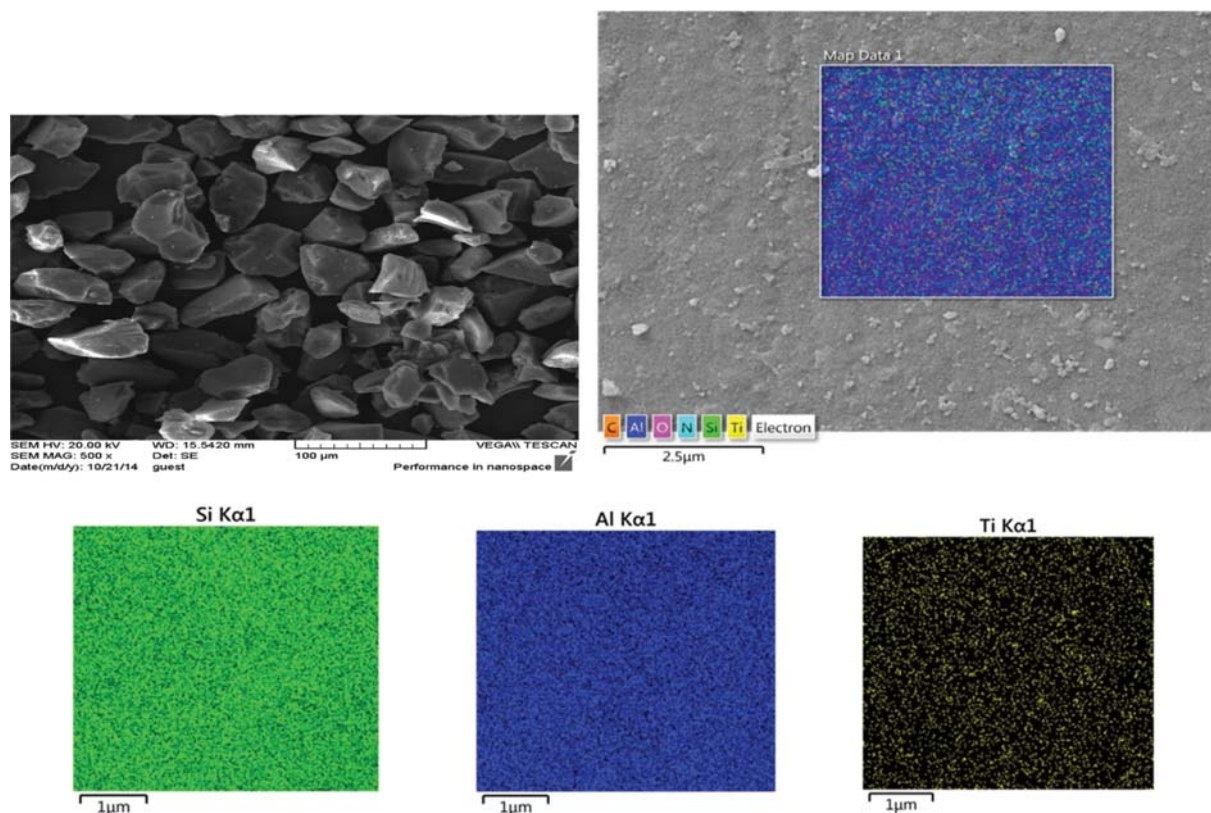


Fig. 5. SEM/elemental mapping images of catalyst sample 5.

for more investigation. Silica support was dried at 350 °C and 600 °C. From another side, in extremely low calcination temperature, the resulting catalyst system may show less activity. Less activity of catalyst at low temperature would be likely attributed to the reaction of hydroxyl groups with catalyst components, which therefore leads to the inactivity of catalyst. But at elevated temperatures, hydroxyl groups on the silica surface are isolated. The constant increase in calcination temperature leads to decrease in the hydroxyl content on the silica surface, and consequently the amount of loading of the precatalyst on support [27-29]. The amount of aluminum in the catalyst decreases with increasing calcination temperature [34].

### 3. Effect of Immobilisation Condition on Catalyst Activity

The immobilization of precatalyst on silica Davisil 643 in different condition and its effect on the activity of catalyst under typical polymerization condition were studied. According to the obtained results, a temperature in the range of 50-70 °C was selected for immobilization. It is assumed that heating facilitates the fixation of precatalyst on the silica, as compared to precatalyst fixation done at 50 °C. It has been reported that higher grafting temperatures lead to the elimination of both (Cl) ligands of the original metallocene and produce bidentate species and lower precatalyst loading. This species should be inactive in polymerization reactions since the absence of a labile ligand (Cl) prevents the formation of the active center which is generated through alkylation of the complex in a reaction with MAO [31]. Increasing the immobilization reaction time from 3 to 18 h led to increase in activity up to 130 Kg poly/

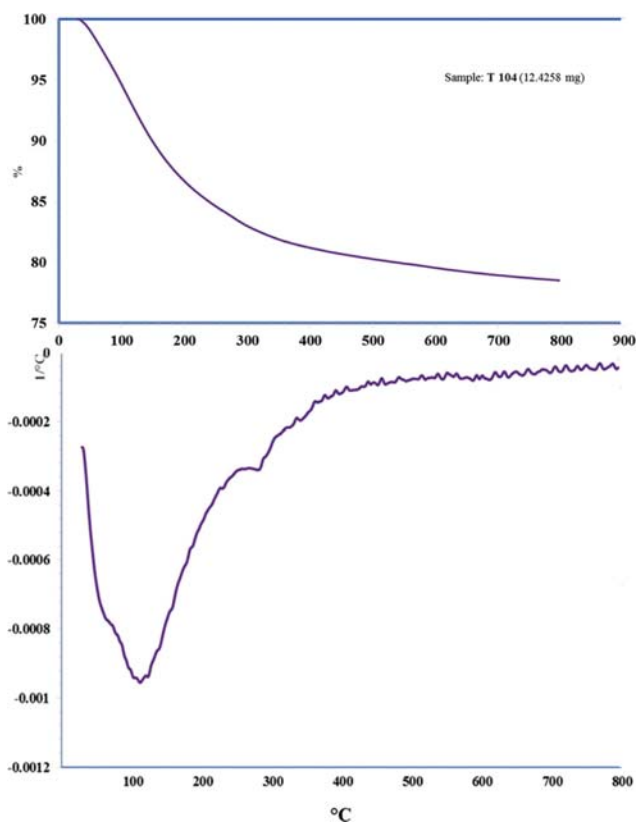


Fig. 6. TGA graph of the catalyst sample 5.

**Table 3. Ethylene homopolymerization with  $(C_5Me_4SiMe_2NtBu)TiCl_2/SiO_2/MAO^a$** 

No.	[Al]/[Ti] (molar ratio)	Temp (°C)	Activity (kg poly/molTi.h.bar)	Bulk density (g/cc)	Crystallinity %	Mw/Mn	Mw $\times(10^{-3})$ (g/mol)
1	190	75	37	0.31	65.84	2.08	823
2	320	75	68	0.31	60.29	2.34	755
3	450	65	73	0.30	51.10	2.14	562
4	450	75	130	0.32	43.82	2.40	693
5	450	80	94	0.32	43.74	2.28	715
6	640	75	156	0.31	43.25	2.55	764
7	770	75	260	0.29	42.68	2.78	874
8	900	75	287	0.31	41.27	2.83	653
9	1160	75	1042	0.30	41.14	2.94	783

<sup>a</sup>Polymerization condition: P=8 bar, t=1 h, immobilization condition: T=60 °C, t=18 h

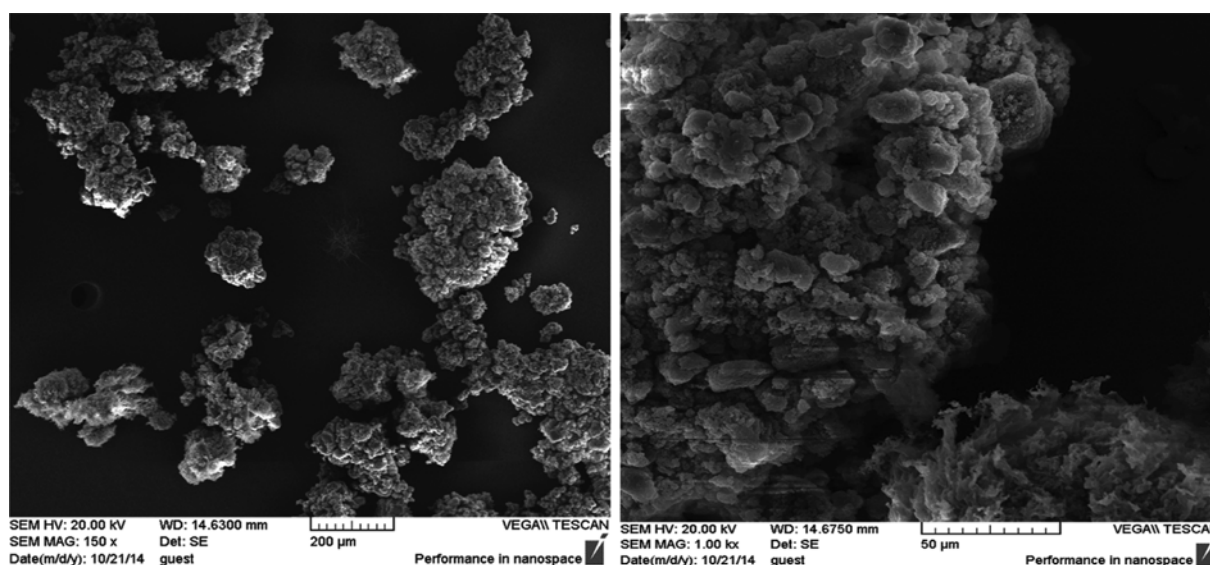


Fig. 7. SEM images of polyethylene sample 4.

mol Ti.h.bar (Table 2). This observation could be most probably attributed to an increase in loading of precatalyst on support.

The SEM and elemental mapping for the catalyst sample 5 with high activity is shown in Fig. 5. It displays the external surface and distribution of Al, Si, and Ti on the catalyst. The morphology remains unchanged from support to the catalyst. It shows clearly that the distribution is essentially random and uniform.

Thermal analysis for the catalyst sample 5 was carried out (Fig. 6). The sample is stable at about 100 °C and above this temperature up to 270 °C with a gentle slope loses about 16% of its weight. Up to 750 °C the catalyst loses its weight with a mild slope and at the end weight loss is 21% of its original weight.

#### 4. Effect of Polymerization Conditions on Ethylene Polymerization Behaviors of CGC Catalyst

Table 3 summarizes the results of ethylene polymerization of catalyst 1 at different conditions. According to Table 3, there is an increase in activity by increasing [Al]/[Ti] ratio. This implies that in this range there is no hindrance of efficient activation of the catalyst with a cocatalyst. The maximum activity of catalyst 1 (1,042 kgPE/mol Ti.bar) with full 1h run appears at 75 °C after raising

[Al]/[Ti] ratio to 1160. As has been reported before for immobilized FI(phenoxy-imin) and CGC systems, the activity of this catalyst was increased to a maximum value as the polymerization increased to 75 °C and then decreased [6,15].

The results indicate that the supported catalyst makes narrow molecular weight distribution polymers. The data in Table 3 show that high bulk density polymers can be prepared from supported catalyst system with various combinations of Al/Ti and temperature. SEM images of polymer sample 4 have been depicted in Fig. 7. It shows that polymer grows and formed clusters. The MAO-treated silica allowed easy access to the monomer in the inner core.

The results extracted from DSC curves showed that in these polymerization condition samples with crystallinity of ~44-66% could be obtained (Table 3). These results are in agreement with the reports related to effective parameters in the formation of branches with CGC catalysts [17].

## CONCLUSIONS

Structural properties of silica support were shown to influence

several parameters and properties of the supported catalyst. Nevertheless, better catalyst activity was obtained with Davisil 643 and Davisil 633, probably due to a more suitable and uniform particle size. Synthesized silica did not afford any advantage in terms of catalyst activity, polymer characteristics. Calcination of support at 350 °C and 600 °C was performed and the results revealed that calcinations at higher temperature lead to systems with higher activity. Synthesis of heterogeneous catalysts was investigated, and the synthesized catalyst showed the highest activity at 60 °C for ethylene polymerization. The time of immobilization of catalyst was evaluated and higher activity was obtained at 18 hours. The catalyst synthesis and polymerization were at different temperatures, and the results showed that the optimum temperature for the polymerization of these systems was 75 °C. With changing the molar ratio of [Al]/[Ti] from 190 to 1160 the activity of catalyst systems changed from 37 to 1,042 (kg poly/molTi.H.bar). The specific morphology of the polymer particles is amorphous with a crystallinity of about 44-66%.

### ACKNOWLEDGEMENTS

The authors would like to express their gratitude to National Petrochemical-Research and Technology Co., of Iran for financial support with grant No. of 870229013.

### REFERENCES

1. D. Arrowsmith, W. Kaminsky, A. M. Schauwienold and U. Weingarten, *J. Mol. Catal. A: Chem.*, **160**, 97 (2000).
2. W. J. Wang, S. Zhu and S. J. Park, *Macromolecules*, **33**, 5770 (2000).
3. M. W. McKittrick and C. W. Jones, *J. Am. Chem. Soc.*, **126**, 3052 (2004).
4. K. Yu, M. W. McKittrick and C. W. Jones, *Organometallics*, **23**, 4089 (2004).
5. M. W. McKittrick, K. Yu and C. W. Jones, *J. Mol. Catal. A: Chem.*, **237**, 26 (2005).
6. J. H. Woo and S. C. Hong, *Polymer-Plastics Technol. Eng.*, **50**, 1557 (2011).
7. J. M. Campos, J. P. Lourenc, H. Cramail and M. R. Ribeiro, *Progress Polym. Sci.*, **37**, 1764 (2012).
8. M. M. Stalzer, M. Delferro and T. J. Marks, *Catal. Lett.*, **145**, 3 (2015).
9. A. Shamiri, M. H. Chakrabarti, S. Jahan, M. A. Hussain, W. Kaminsky, P. V. Aravind and W. A. Yehye, *Materials*, **7**, 5069 (2014).
10. P. J. Sinnema, B. Hessen and J. H. Teuben, *Macromol. Rapid Commun.*, **21**, 562 (2000).
11. A. Eisenhardt and W. Kaminsky, *Catal. Commun.*, **5**, 653 (2004).
12. P. Kaivalchatchawal, P. Praserttham, Y. Sogo, Z. Cai, T. Shiono and B. Jongsomjit, *Molecules*, **16**, 4122 (2011).
13. S. Mehdiabadi and J. B. P. Soares, *Macromolecules*, **45**, 1777 (2012).
14. S. Guo, H. Fan, Z. Bu, B. G. Li and S. Zhu, *Macromol. React. Eng.*, **9**, 32 (2015).
15. J. Chai, K. A. Abboud and S. A. Miller, *Dalton Trans.*, **42**, 9139 (2013).
16. I. V. Sedov, V. D. Makhaev and P. E. Matkovskii, *Catal. Ind.*, **4**, 129 (2012).
17. P. Liu, W. Liu, W. J. Wang, B. G. Li and S. Zhu, *Macromol. React. Eng.*, **10**, 156 (2016).
18. B. Yang, M. Yang, W. J. Wang and S. Zhu, *Polym. Eng. Sci.*, **52**, 21 (2012).
19. E. Kolodka, W. J. Wang, S. Zhu and A. Hamielec, *Macromol. Rapid Commun.*, **24**, 311 (2003).
20. W. J. Wang, D. Yan, S. Zhu and A. E. Hamielec, *Macromolecules*, **31**, 8683 (1998).
21. F. Pradest, J. P. Broyet, I. Belaid, O. Boyron, O. Miserque, R. Spitz and C. Boisson, *ACS Catal.*, **3**, 2288 (2013).
22. M. A. Bashir, T. Vancompern, R. M. Gauvin, L. Delevoye, N. Merle, V. Monteil, M. Taoufik, T. F. L. McKenna and C. Boisson, *Catal. Sci. Technol.*, **6**, 2962 (2016).
23. J. S. Oh, B. Y. Lee and T. H. Park, *Korean J. Chem. Eng.*, **21**, 110 (2004).
24. S. Y. Lee and K. Y. Choi, *Macromol. React. Eng.*, **8**, 755 (2014).
25. J. S. Chung, G. Tairova, Y. Zhang, J. C. Hsu, K. B. McAuley and D. W. Bacon, *Korean J. Chem. Eng.*, **19**, 597 (2002).
26. S. Y. Lee, J. S. Lee and Y. S. Ko, *Korean Chem. Eng. Res.*, **53**, 397 (2015).
27. J. C. Stevens, F. J. Timmers, D. R. Wilson, G. F. Schmidt, P. N. Nickias, R. K. Rosen, G. W. Knight and S. Y. Lai, EP Patent 0, 416, 815 A2 (1991).
28. A. C. dos Ouros, M. O. de Souza and H. O. Pastore, *J. Brazilian Chem. Soc.*, **25**, 2164 (2014).
29. F. Silveira, C. F. Petry, D. Pozebon, S. B. Pergher, C. Detoni, F. C. Stedile and J. H. Z. dos Santos, *Appl. Catal. A: Gen.*, **1**, 96 (2007).
30. S. Music, N. F. Vincekovic and L. Sekovanic, *Brazilian J. Chem. Eng.*, **28**, 89 (2011).
31. J. H. Z. dos Santos, C. Krug, M. B. da Rosa, F. C. Stedile, J. Dupont and M. de C. Forte, *J. Mol. Catal. A: Chem.*, **139**, 199 (1999).
32. M. Atiqullah, M. N. Aktar, A. A. Moman, A. H. Abu-Roqabah, S. J. Palackal, H. A. Al-Muallem and O. M. Hamed, *Appl. Catal. A: Gen.*, **320**, 134 (2007).
33. Tailor-Made Polymers via Immobilization of Alpha-olefin Polymerization Catalysts, Edited by John R. Severn and John C. Chadwick, Copyright 2008 WILEY-VCH Verlag GmbH & Co., KGaA, Weinheim.
34. M. A. Bashir, T. Vancompernelle, R. M. Gauvin, L. Delevoye, N. Merle, V. Monteil, M. Taoufik, T. F. McKenna and C. Boisson, *Catal. Sci. Technol.*, **6**, 2962 (2016).